



Thermodynamic and Adsorption Studies of Corrosion Inhibition of Mild Steel Using Lignin from Siam Weed (*Chromolaena odorata*) in Acid Medium

F. O. Nwosu^{a*}, M. M. Muzakir^b

^aDepartment of Chemistry, Faculty of Physical Sciences, University of Ilorin, P. M. B. 1515, Ilorin, Nigeria

^bDepartment of Chemistry, Faculty of Science, Gombe State University, P. M. B. 127, Gombe, Nigeria.

Received 12 Feb 2015, Revised 14 Jan 2016, Accepted 22 Jan 2016

*Corresponding author: E-mail: f.o.nwosu@gmail.com (F. O. Nwosu); Phone: +2348035819766.

Abstract

Corrosion has been chronic problem to industries and has increased cost of production. Lignin is the second most natural organic polymer on the earth and it can be obtained from the wastes of wood pulping processing in the form of black liquor. The inhibition efficiency of lignin on the corrosion of mild steel in 1 M HCl have been evaluated by conventional weight loss method, and surface analysis using 500-5000 mg/L (w/v) inhibitor concentration in temperature range of 303-343 K. Maximum inhibition efficiency of 92.39 % was obtained with optimum inhibitor concentration of 4000 mg/L at 303 K. The activation and free energies for the inhibition reactions support the mechanism of physical adsorption. The adsorption of lignin extract on mild steel surface is endothermic, spontaneous and consistent with the Langmuir adsorption isotherm at all studied temperatures. FT-IR and SEM analyses confirmed that the surface of mild steel was affected by the adsorption of lignin onto the surface to form ferric-lignin compounds.

Keywords: Lignin, Corrosion inhibition, Mild steel, Thermodynamic parameters, Adsorption.

1. Introduction

Corrosion is a natural phenomenon, which can be considered either chemical or electrochemical in nature, degrades the metallic properties of metal and alloys and make them unfit for specific role. Corrosion of metals is a major industrial problem that has attracted much investigations and researches. This is because some industrial processes such as acid cleaning, pickling and descaling facilitate contact between metal and aggressive medium (such as acid, base or salt), consequently the metal is prone to corrosion. In order to reduce the menace due to corrosion of industrial installations, several steps have been adopted.

However, one of the best options available for protecting metals against corrosion involves the use of corrosion inhibitors. Corrosion inhibitors are widely used in industry to reduce the corrosion rate of metals and alloys in contact with aggressive environment [1]. Circulating cooling water system is a commonly used instrument in industry. Two of the main operating problems of the cooling water system are corrosion and scale formation because of the electrochemical oxidation reduction reaction and the metal salt sediments on the metal surface [2].

Though many synthetic compounds such as chromium (III) and cerium (IV) oxides, cerium (III) chloride, 8-hydroxyquinoline, benzotriazole, 2-mercaptobenzothiazole (MBT), mercaptobenzimidazole (MBI) and some monosaccharide derivatives showed good anti-corrosive activity, most of them are highly toxic to both human and environment [3-4]. The safety and environmental issues of corrosion inhibitors arisen in industries has always been a global concern. These inhibitors may cause reversible (temporary) or irreversible (permanent) damage to organ system viz, kidneys or liver, or to disturb a biochemical process or an enzyme

system at some site in the body [5]. Therefore, it is desirable to source for environmentally safe corrosion inhibitors.

The exploration of natural products of plant origin as inexpensive and eco-friendly corrosion inhibitors is an essential field of study. In addition to being environmentally friendly and ecologically acceptable, plant products are biodegradable, low-cost, readily available and renewable sources of materials. Perhaps, the most common natural substances used are plant extracts, such as *Rosmarinus officinalis* [6], fruits of *Terminalia chebula* [7], *Cassia auriculata* extract [8], cannabis extract [9], *Parthenium hysterophorus* extract [10], *Gnetum africana* leaves extract [11], *Albizia lebbek* seed extract [12], Argan extract [13], *Bucolzia coriacea* and *Cninodoscolus chayansa* [14], *Calotropis* extract [15], *Alstonia boonei* extract [16], *Damsissa* and *Corchours itorius* extracts [17], *Treculia africana* leaves extract [18], fenugreek leaves and lemon peel extract [19], Anise extract [20]. Some essential oil has also been used [21-22]. Generally, these various plant extracts contain compounds having heteroatoms such as O, N and S which exhibit basicity and electron density that assist in corrosion inhibition. O, N and S are active centers for adsorption on the metal surface [15]. Lignin may be the second most abundant natural organic polymer on earth, it is a heterogeneous biopolymer and a chemical compound that is an integral part of plant cell walls which provides the mechanical strength of plants cellulose and it is assembled from coniferyl alcohol type monomers by enzymatic polymerization providing a three-dimensional molecular architecture [23].

Chemical structures of the precursors are presented in figure 1. Lignin can be acquired from the wastes of wood pulping processing in the form of black liquor. This study investigates the corrosion inhibition of mild steel by lignin extracted from the stem of Siam weed (*Chromolaena odorata*) in 1 M HCl using weight loss method complemented by FT-IR and SEM. The use of leave extract of *Chromolaena odorata* has been utilized as inhibitor but to the best of our knowledge no reported literature is available for using lignin extract of *Chromolaena odorata* for corrosion inhibition of mild steel in hydrochloric acid medium.

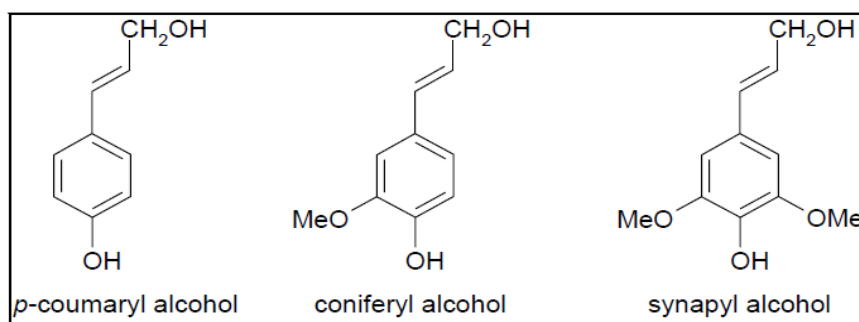


Figure 1: The major building blocks of lignin

2. Experimental

2.1 Materials Preparation

Mild steel sheet was obtained commercially. The used mild steel coupons have percent composition (% wt.) of 98.79 % Fe, 0.15 % C, 0.63 % Mn, 0.07 % S and 0.36 % P. The surface preparation of mild steel coupons (3 cm x 2 cm x 0.12 cm) was carried out with emery papers by increasing grades (200, 400 and 600 grit sizes), then degreased with AR grade ethanol and dried at room temperature ; and stored in moisture free desiccators before their use in corrosion studies [24]

2.2 Extraction of lignin

A weighed amount of the powdered sample of *Chromolaena odorata* stems was placed in a round bottom flask, 5 M NaOH solution was charged into the flask, in the ratio of 1: 10 (solid : liquid). The flask was equipped with a condenser and heated at 100 °C for 7 hours. The mixture was filtered and the filtrate (black liquor) was precipitated with 50 % H₂SO₄ solution to pH 2 and was filtered again. The residue which is the lignin was

washed with acidified water (pH 2) several times. The lignin cake was then sucked dry under vacuum and finally dried in an oven at 50 °C for 2 hours [23].

2.3 Solution preparation

A stock solution of 1 M HCl was prepared from 35.4 % HCl using deionized water. This was used as solvent to prepare the lignin concentration by w/v in the range of 500-5000 mg/L.

2.4 Weight loss measurements

Experiments were performed at 30, 40, 50, 60, and 70 °C in blank HCl and with different concentrations of lignin extract. The immersion time for the weight loss measurements is 5 hours after which the coupon specimens of steel were carefully washed in double-distilled water, dried and then weighed [24] using Mettler Toledo XS64 electronic weighing balance with the accuracy of ± 0.0001 g. All experiments are in triplicates and illustrated data are mean values of obtained results. From the average weight loss, the corrosion rate (CR), inhibition efficiency (IE) and surface coverage (θ) were calculated using equations 1, 2 and 3 respectively [25, 26].

$$CR (mgcm^{-2}h^{-1}) = \frac{W}{At} \quad (1)$$

$$IE (\%) = \frac{W_1 - W_2}{W_1} \times 100 \quad (2)$$

$$\theta = \frac{W_1 - W_2}{W_1} \times 100 \quad (3)$$

Where W is weight loss (mg), A is the exposed area (cm²) and t is the immersion time (h), W₁ and W₂ are the weight loss of mild steel in absence and presence of inhibitor respectively.

2.5 Surface analysis

Scanning Electron Microscope (FEI NOVA NANOSEM 230), which was equipped with an energy dispersive X-ray microanalysis (EDX) system (FEI, Eindhoven, Holland) was used to study the morphology and chemical analysis of the corroded mild steel surfaces. FT-IR spectroscopy (Shimadzu 8400 FTIR spectrometer) was used to collect the IR spectra of the dried lignin sample as well as the mild steel corrosion product in the presence of optimum concentration of lignin.

3. Results and Discussion

3.1 Effect of concentration and temperature

The corrosion rate and inhibition efficiency for mild steel in 1M HCl solution at 30, 40, 50, 60 and 70 °C in the absence and presence of lignin extract are given in Table 1. The corrosion rate (CR) is higher in the uninhibited solutions compared to the inhibited; which is as a result of the mitigating effect of the lignin on the corrosion rate of mild steel. The corrosion rate decreases as the concentration of lignin extract increases to 4000 mg/L. This suggests that as the concentration of the extract increases, there is an increase in the number of adsorption of the extract constituents onto the surface of the mild steel which makes a barrier for mass transfer and prevents further corrosion.

However, the inhibition efficiency increases with increase in concentration of the lignin. This is attributed to the increase in the fraction of the mild steel surface covered (θ) by the adsorbed constituents of the lignin as the concentration of the lignin increases. The inhibition efficiency increases progressively as the concentration of lignin increases up to 4000 mg/L. However, further increase in lignin concentration did not cause any increase in the inhibition efficiency, rather the inhibition efficiency remains constant or decreases slightly in some cases.

This might indicate that the reaction of the inhibitor on the surface of the mild steel has reached the state of equilibrium. These results are similar to the findings reported in literature [27]. Maximum inhibition efficiency of 86.68 % was found at 50 °C (323 K) with 4000 mg/L lignin concentration.

Table 1: Corrosion parameters of mild steel in 1 M HCl in various concentrations of lignin extract at various temperatures

Temperature (K)	Inhibitor concentration (mg L ⁻¹)	WL (mg)	CR (mg cm ² h ⁻¹)	θ	IE (%)
303	Uninhibited	38.10	0.635	-	-
	500	13.70	0.228	0.6404	64.04
	1000	12.95	0.216	0.6601	66.01
	2000	11.50	0.192	0.6982	69.82
	3000	11.00	0.183	0.7113	71.13
	4000	9.60	0.160	0.7480	74.80
	5000	9.60	0.160	0.7480	74.80
313	Uninhibited	96.50	1.608	-	-
	500	32.05	0.534	0.6679	66.79
	1000	28.55	0.476	0.7041	70.41
	2000	27.50	0.458	0.7150	71.50
	3000	22.50	0.375	0.7668	76.68
	4000	20.35	0.339	0.7891	78.91
	5000	21.60	0.360	0.7792	77.92
323	Uninhibited	235.30	3.922	-	-
	500	64.35	1.073	0.7265	72.65
	1000	57.40	0.957	0.7561	75.61
	2000	43.10	0.718	0.8168	81.68
	3000	35.30	0.588	0.8499	84.99
	4000	31.35	0.523	0.8668	86.68
	5000	31.45	0.524	0.8663	86.63
333	Uninhibited	398.50	6.642	-	-
	500	141.50	2.358	0.6449	64.49
	1000	102.50	1.708	0.7428	74.28
	2000	72.50	1.208	0.8181	81.81
	3000	62.50	1.042	0.8432	84.32
	4000	60.50	1.008	0.8482	84.82
	5000	55.00	0.917	0.8619	86.19
343	Uninhibited	950.50	15.842	-	-
	500	511.50	8.525	0.4619	46.19
	1000	346.50	5.775	0.6355	63.55
	2000	189.50	3.158	0.8006	80.06
	3000	160.00	2.667	0.8317	83.17
	4000	136.05	2.268	0.8569	85.69
	5000	136.05	2.268	0.8569	85.69

It was observed that the CR of mild steel in uninhibited and in the presence of lignin extract increases with increase in temperature. This is as a result of increase in the average kinetic energy of the reacting molecules. The variation of inhibition efficiency (IE) with temperature did not follow a consistent trend as in the case of corrosion rate. The IE increases as the temperature increase from 30 to 50 °C and then decreases

slightly as the temperature increases from 50 to 70 °C. Improvement in inhibition efficiency with increasing temperature is attributed to a change in the nature of adsorption, wherein the inhibitor is physically adsorbed at lower temperature while chemisorption is favoured at higher temperature [11].

3.2 Effect of acid concentration

The effect of HCl concentration on CR and IE was studied in uninhibited and in the presence of optimum concentration (4000 mg/L) of lignin. The HCl concentration was varied in the range of 0.5-2.5 M. The results are presented in Table 2. The CR was observed to increase with increase in concentration of HCl in both the uninhibited and inhibited solutions. This observation is due to the fact that the rate of chemical reaction increases as the concentration of active species increases [28]. The IE was found to decrease from 84.62 % to 72.22 % as the concentration of HCl increases from 0.5 to 2.5 M. This can be attributed to the increase in number of chloride ions at the steel surface as the concentration of HCl increases which hinder the adsorption of the lignin molecules onto the steel surface thereby decreasing the inhibition efficiency. Similar observation has been reported in literature [29].

Table 2: Corrosion parameters of mild steel in different concentrations of uninhibited HCl and with 4000 mg/L of lignin extract at 303 K.

[HCl]	WL (mg)		CR (mg cm ⁻² h ⁻¹)		θ	IE (%)
	Uninhibited Solution	Inhibited Solution	Uninhibited Solution	Inhibited Solution		
0.5	13.0	2.0	0.217	0.033	0.8462	84.62
1.0	27.0	5.0	0.450	0.083	0.8148	81.48
1.5	34.0	7.0	0.567	0.117	0.7941	79.41
2.0	47.0	12.0	0.783	0.200	0.7447	74.47
2.5	54.0	15.0	0.900	0.250	0.7222	72.22

3.3 Effect of immersion time

The results of effect of immersion time on CR and IE are shown in Table 3. The CR and IE were calculated at 5 days interval for the total period of 30 days in uninhibited HCl and in the presence of optimum concentration of lignin (4000 mg/L) at 303 K. The corrosion rate decreases as the immersion time increases to 20 days and then increases after 30 days of immersion. The continuous decrease in corrosion rate could be attributed to the formation of oxide film which shields the mild steel surface from having direct contact with the acidic environment and the later increase could be due to the destruction of the oxide film formed on the mild steel surface by the chloride ions [30]. The inhibition efficiency also decreases from 92.39 % after 5 days of immersion to 61.70 % after 30 days immersion time. Similar trend has also been reported by other researchers [12]. This indicates the effectiveness of lignin in reducing the corrosion of mild steel in 1 M HCl solution even after 30 days of immersion by 61.70 %.

Table 3: Corrosion parameters of mild steel in uninhibited 1 M HCl and with optimum concentration of lignin (4000 mg/L) at different immersion time at 303 K

Immersion time (days)	WL (mg)		CR (mg cm ⁻² h ⁻¹)		θ	IE (%)
	Uninhibited Solution	Inhibited Solution	Uninhibited Solution	Inhibited Solution		
5	1039	79	0.722	0.055	0.9239	92.39
10	985	156	0.342	0.054	0.8416	84.16
15	915	234	0.212	0.054	0.7443	74.43
20	857	423	0.149	0.073	0.5064	50.64
25	1987	596	0.230	0.083	0.7036	70.36
30	2011	761	0.279	0.088	0.6170	61.70

3.4 Adsorption isotherm and thermodynamic studies

Adsorption isotherms are very important in determining the mechanism of organo electrochemical reaction. The effectiveness of organic compounds as corrosion inhibitors can be ascribed to the adsorption of molecules of the inhibitors through their polar functions on the metal surface. The metal surface in aqueous solution is always covered with adsorbed water dipoles. Therefore, the adsorption of inhibitor molecules from aqueous solution is a quasi substitution process [25]. In order to consider the adsorption process of lignin on the steel surface, Langmuir adsorption isotherm was tested according to equation 4 [31].

$$\text{Langmuir: } \frac{C_{inh}}{\theta} = \frac{1}{K_{ads}} + C_{inh} \quad (4)$$

Where θ is the surface coverage, K_{ads} is the equilibrium constant of the adsorption, C_{inh} is the inhibitor equilibrium concentration. The experimental data were best described by Langmuir isotherm with the highest regression coefficient, R^2 close to 1 as shown in Table 4. The departure in the values of the slopes of Langmuir plots from unity may be advocated to be due to the mutual repulsion or attraction between the adsorbed molecules in close vicinity which may affect the heat of adsorption [32]. A modified Langmuir adsorption isotherm [33], given by the corrected equation as follows, could be applied to this phenomenon.

$$\frac{C_{inh}}{\theta} = \frac{n}{K_{ads}} + nC_{inh} \quad (5)$$

The K_{ads} values were calculated from the intercept lines on the C_{inh}/θ axis (Fig.2). This is related to the free energy change of adsorption (ΔG_{ads}) as reported elsewhere [23].

$$\Delta G_{ads} = -2.303RT(55.5 \text{ Log } K_{ads}) \quad (6)$$

Where 55.5 is the water concentration of the solution mL/L.

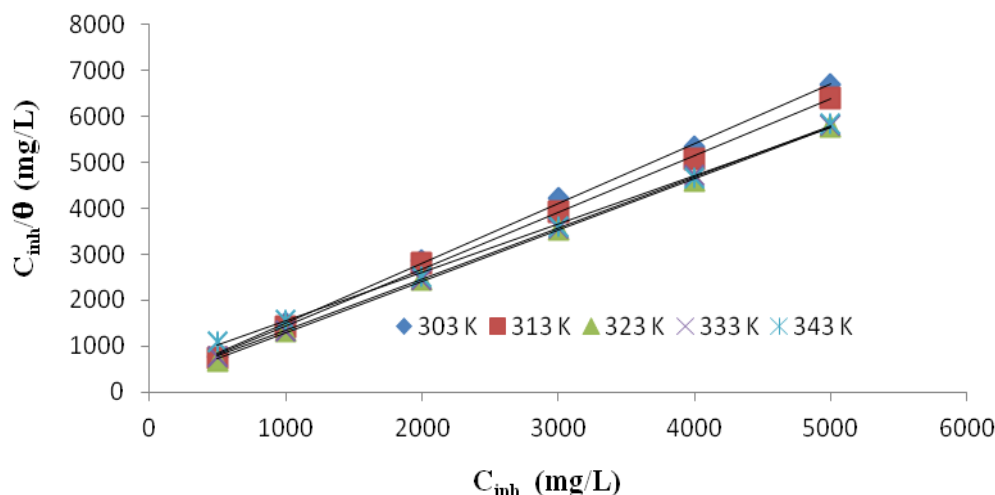


Figure 2: Langmuir adsorption isotherm plots for mild steel in 1 M HCl with different concentrations of lignin extract at different temperatures.

Since the natural extract contains infinite compounds at various contents, we assume that the inhibition process is essentially due to the synergistic intermolecular phenomenon between molecules of natural product at major levels [25].

The activation energy (E_a) values were determined from Arrhenius plots for mild steel corrosion by the following relation [25]:

$$\text{Log } CR = \text{Log } A - \frac{E_a}{2.303RT} \quad (7)$$

Where A is the Arrhenius pre-exponential constant, T is the absolute temperature (K) and R is the universal gas constant (8.314 J/mol K).

The Ea values as shown in Table 5 are lower in inhibited solutions compared to the uninhibited hence leading to reduction in the corrosion rates which suggest that, lignin molecules are strongly adsorbed onto the steel surface [34].

Table 4: Langmuir isotherm and Free Energy change parameters for lignin on Mild steel in 1 M HCl obtained at different temperatures.

Temperature (K)	K_{ads} (mol^{-1})	n	R^2	ΔG_{ads} (kJ/mol)
303	206.54	1.301	0.999	-23.55
313	187.27	1.241	0.9988	-24.07
323	174.89	1.118	0.9997	-24.66
333	217.52	1.119	0.9999	-26.03
343	490.64	1.053	0.9986	-29.13

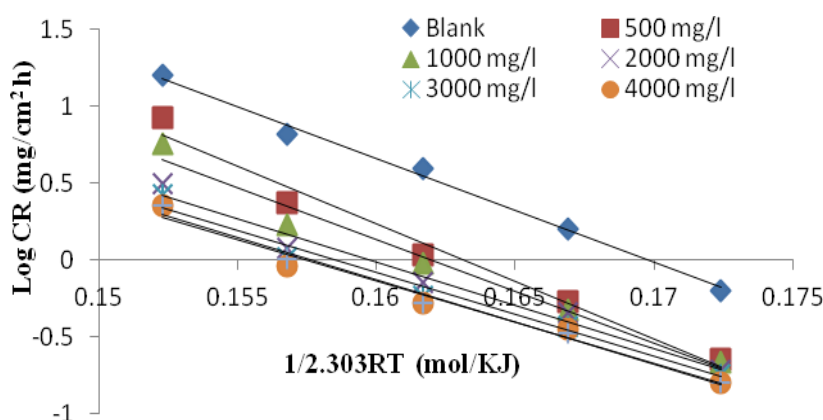


Figure 3: Arrhenius plots for mild steel in 1 M HCl solution in the absence and presence of various concentrations of lignin

The transition state equation for dissolution or adsorption process as reported elsewhere [25] is given by equation 8.

$$\text{Log} \left(\frac{CR}{T} \right) = \left[\text{Log} \left(\frac{R}{hN} \right) + \left(\frac{\Delta S_{ads}}{2.303R} \right) \right] - \frac{\Delta H_{ads}}{2.303RT} \quad (8)$$

Where h is the Planck's constant (6.6261×10^{-34} Js), N is Avogadro's number ($6.0225 \times 10^{23} \text{ mol}^{-1}$). From the plot of $\log = \left(\frac{CR}{T} \right)$ against $\frac{1}{T}$, enthalpy change (ΔH_{ads}) and entropy change (ΔS_{ads}) of adsorption were estimated from the slope and intercept respectively. The values of (ΔH_{ads}) and (ΔS_{ads}) are presented in Table 5. The positive values of (ΔH_{ads}) reflect the endothermic nature of steel dissolution process. It is well noticed that the values of Ea are larger than the analogous values of (ΔH_{ads}) indicating that the corrosion process might have involved a gaseous reaction, like the hydrogen evolution reaction, associated with a decrease in the total reaction volume [25].

The negative values of ΔS_{ads} showed that the activated complex in the rate determining step represents an association rather than a dissociation step. It is clear from data listed in Table 5 that ΔS_{ads} decreased in value in the presence of lignin compared to uninhibited acid. In uninhibited solutions the transition state of the rate determining recombination step represents a more orderly arrangement relative to the initial state, so a high value for the entropy of activation is obtained. In the presence of lignin, however, the rate determining step is the discharge of hydrogen ions to form adsorbed hydrogen atoms. Since the surface is covered with lignin molecules, this will retard the discharge of hydrogen ions at the metal surface causing the system to pass from a random arrangement, and hence entropy of activation is decreased.

The decreased of ΔS_{ads} with increasing inhibitor concentration, reveals that a decrease in disordering takes place on going from reactant to the activated complex. This behavior can be explained as a result of the replacement process of water molecules during adsorption of lignin molecules onto the mild steel surface [35].

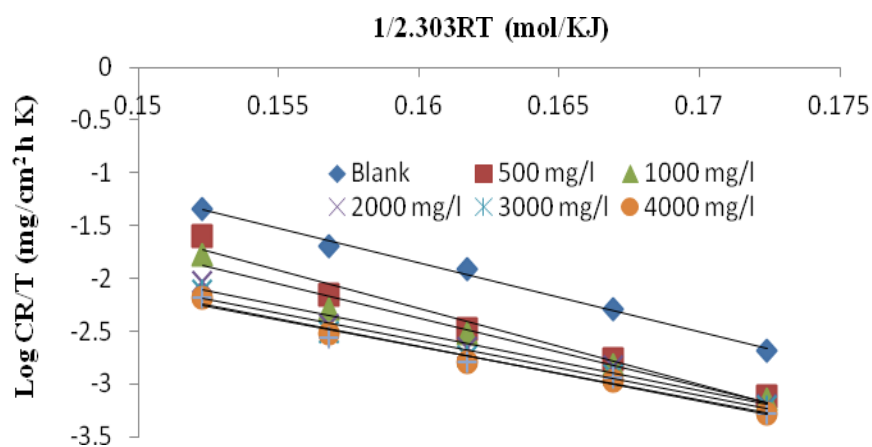


Figure 4: Transition state plots for mild steel in 1 M HCl solution in the absence and presence of various concentrations of lignin

Table 5: Activation parameters of the dissolution of mild steel in uninhibited 1 M HCl and in the presence of different concentrations of lignin.

Inhibitor concentration (mg L ⁻¹)	E_a (kJmol ⁻¹)	R^2	ΔH_{ads} (kJmol ⁻¹)	ΔS_{ads} (Jmol ⁻¹ K ⁻¹)	R^2
Uninhibited	67.82	0.9948	65.15	-33.47	0.9943
500	74.97	0.9772	72.30	-19.71	0.9757
1000	67.45	0.976	64.78	-44.71	0.9742
2000	56.56	0.9776	53.88	-80.84	0.9756
3000	54.83	0.9771	52.16	-87.44	0.9749
4000	53.66	0.9756	52.34	-87.79	0.9849
5000	55.01	0.9861	50.99	-92.03	0.9733

3.5. FT-IR analysis

The FT-IR spectrum of lignin is shown in Fig. 5a. Phenolic -OH stretching appeared at 3416 cm⁻¹. The peak at 2920 cm⁻¹ can be assigned to aromatic C-H. The aromatic C=C stretching frequency appeared at 1639 cm⁻¹ while the value of 1728 cm⁻¹ suggest C=O stretching frequency. The peaks at 1508 and 1421 cm⁻¹ can be assigned to aromatic rings due to aromatic skeletal vibrations. The peak at 1329 cm⁻¹ is due to bending vibrations of OH groups and 1209 cm⁻¹ is due to guaiacyl ring breathing with C-O stretching. The FT-IR

spectrum of the protective film formed on the surface of the steel after immersion is shown in Fig. 5b. It was found that, some of the peaks observed for lignin are also noticed for the mild steel immersed in 1 M HCl containing 4000 mg/L of lignin extract. Phenolic -OH stretching has shifted from 3416 to 3362 cm^{-1} . The aromatic C-H stretching shifted from 2920 to 2360 cm^{-1} . The aromatic rings vibration also fell within the same range of 1421 - 1413 cm^{-1} . The bands at 829 and 466 cm^{-1} probably originate mainly from α -FeOOH and γ -Fe₂O₃ respectively [25].

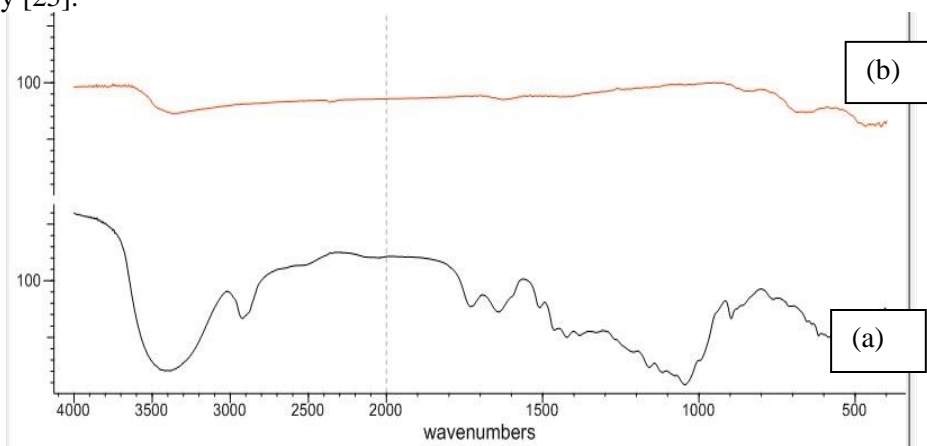


Figure 5: FT-IR spectra: (a) dried lignin extract; (b) Film formed on steel surface after 48 h of immersion in 1 M HCl + 4000 mg/L lignin extract at 30 °C.

3.6 Surface morphology analysis

Scanning electron microscope (SEM) images were taken in order to study the surface morphology of mild steel in absence and presence of lignin inhibitor. SEM image (Fig. 6a) reveals that in the absence of lignin extract, the mild steel surface is highly damaged with pitted areas. This shape is typical to pitting corrosion [25].

Fig. 6b shows a smooth surface with deposited lignin extract on it for the specimen after immersion in 1M HCl solution containing 4000 mg/L lignin extract. By comparison of SEM images at the same magnifications (500 X), it is indicated that the pits disappear and mild steel is almost free from corrosion in HCl with lignin extract. This is because of the formation of an adsorbed film of lignin molecules inhibiting the pitting corrosion of mild steel in 1 M HCl solution.

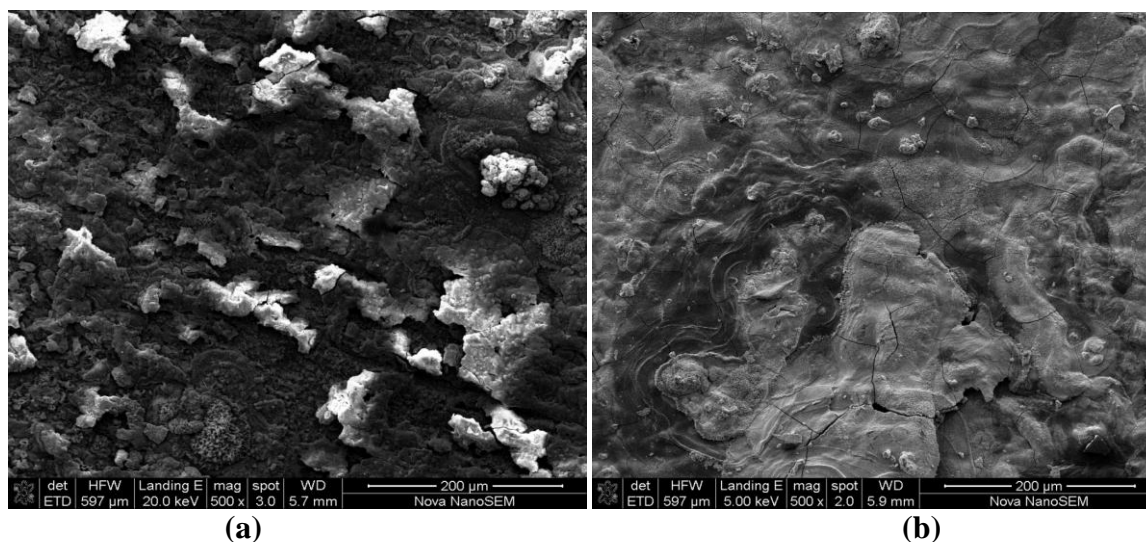


Figure 6: SEM micrographs for surface of mild steel specimens after 48 h of immersion in 1 M HCl solution: (a) without lignin extract; (b) with 4000 mg/L lignin extract at 30 °C.

Conclusion

It was found that inhibition efficiency increases with increasing lignin concentration and temperature to 323 K, but decreases with increase in HCl concentration. Activation energies were lower in the presence of the lignin extract and decreases as the inhibitor concentration increases suggesting a decrease in corrosion rate of mild steel while Gibb's free energy, enthalpy and entropy of adsorption indicate that the adsorption process is spontaneous and endothermic in nature. The SEM and Langmuir adsorption isotherm studies suggested that the mechanism of corrosion inhibition occurred through adsorption process.

References

1. Rajendran A., Karthikeyan C., *Int. J. Plant Res.* 2 (2012) 9.
2. Defang Z., Wen Q., *J. Surf. Eng. Mater. Adv. Technol.* 2 (2012) 137.
3. Ismaily Alaoui K., El Hajjaji F., Azaroual M. A., Taleb M., Chetouani A., Hammouti B., Abridgach F., Khoutoul M., Abboud Y., Aouniti A., Touzani R., *J. Chem. Pharmac. Res.*, 6 N^o7 (2014) 63-81
4. Methal A., Koulou A., El Bakri M., Ebn Touhami M., Galai M., Lakhrissi M., Tourir R., Bakkali S., *Maghr. J. Pure & Appl. Sci.* 1 (2015) 46.
5. Singh A., Quraishi M. A., *J. Chem. Pharm. Res.* 4 (2012) 322.
6. Velázquez-González M. A., Gonzalez-Rodriguez J. G., Valladares-Cisneros M. G., Hermoso-Diaz I. A., *American Journal of Analytical Chemistry*, 5 (2014) 55.
7. Deepa P., Padmalatha R., *J. Mater. Environ. Sci.* 6(2015) 412.
8. Rosaline J.V., Leema A. R., Raja S., *Int. J. Chem. Tech. Res.* 3 (2011) 1791.
9. El-Housseiny S., Abd-El-Nabey B. A., Abdel-Gaber A. M., El- Said A. M., Khamis E., *Int. J. Electrochem Sci.* 7 (2012)11811.
10. Prakash R., Ji G., Shukla S. K., Dwivedi P., Sundaram S., Ebenso E.E., *Int. J. Electrochem. Sci.* 7 (2012) 9933.
11. Nnanna L. A., Owate I. O., Nwadiuko O. C., Ekekwe N. D., Oji W. J., *Int. J. Mater. Chem.* 3 (2013) 10.
12. Arumugam P., Subbiah S., Kannusamy K., *Biointer. Res. Appl. Chem.* 3 (2012) 498.
13. Afia L., Salghi R., Bammou L., Bazzi L. h., Hammouti B., Bazzi L., *Acta Metall. Sin. (Engl. Lett.)* 25 (2012) 10.
14. Akalezi C. O., Ogukwe C. E., Enenebaku C. K., Oguzie E. E., *Environ. Pollu.* 1 (2012) 45.
15. Kumar S., Mathur S. P., *Internationally Research Notices* (2013) 1
16. Ituen E. B., Udo U. E., Odozi N. W., Dan E. U., *IOSR J. Appl. Chem.* 3 (2013) 52.
17. Abd-El-Nabey B.A., Abdel-Gaber A.M., Elawady G.Y., El-Housseiny S., *Int. J. Electrochem. Sci.* 7 (2012) 7823.
18. Ejikeme P.M., Umana S.G., Onukwuli O.D., *Port. Electrochim. Acta* 30 (2012) 317.
19. Agarwal K., *J. Mater. Sci. Surf. Eng.* 1 (2014) 44.
20. Fouda A. S., Elewady G. Y., shalabi K., Habouba S., *International Journal of Innovative Research in Science, Engineering and Technology*, 3 (2014) 11210.
21. El Ouadi Y., Lahhit N., Bouyanzer A., Majidi L., Elmsellem H., Cherrak K., Elyoussfi A., Hammouti B., Costa J., *Arabian Journal of Chemical and Environmental Researches* 1 (2015) 1.
22. Lgaz H., Belkhaouda M., Larouj M. , Salghi R., Jodeh S. , Warad I., Oudda H., Chetouani A., *Mor. J. Chem.* 4 (2016) 101.
23. Akbarzadeh E., Ibrahim M. M. N., Abdul Rahim A., *Int. J. Electrochem. Sci.* 6 (2011) 5396.
24. Manssouri M., El Ouadi Y., Znini M., Costa J., Bouyanzer A. Desjobert J-M., Majidi L., *J. Mater. Environ. Sci.* 6 (2015) 631.
25. Andreani S., Znini M., Paolini J., Majidi L., Hammouti B., Costa J., Muselli A. , *J. Mater. Environ. Sci.* (2016) 187-195

26. Olasehinde E. F., Olusegun S. J., Adesina A. S., Omogbehin S. A., Momoh-Yahayah H., *Natature and Science*, 11 (2013) 83.
27. Shyamala M., Kasthuri P. K., *Int. J. Corros.* (2012) 1.
28. Uzoma O. T., Maryjane I. I., Thompson U. E., Egbulefu I. A. V., Lilian U. N., *J. Chem. Chem. Eng.* 6 (2012) 708.
29. Abd-El-Khalek D. E., Abd-El-Nabey B. A., Abdel-Gaber A. M., *Port. Electrochim. Acta* 30 (2012) 247.
30. Ikpeseni S. C., *J. Sci. Multidisciplinary Res.* 4 (2012) 10.
31. Benali O., Benmehdi H., Hasnaoui O., Selles C., Salghi R., *J. Mater. Environ. Sci.* 4 (2013) 127.
32. Yadav M., Sharma U., *J. Mater. Environ. Sci.* 2 (2011) 407.
33. Hammouti B., Patel N. S., Jauhariand S., Mehta G. N., Al-Deyab S. S., Warad I., *Int. J. Electrochem. Sci.* 8 (2013) 2635.
34. Umoren S. A., Obot I. B., Obi-Egbedi N. O., *J. Mater. Environ. Sci.* 2 (2011) 60.
35. Dahmani M., Et-Touhami A., Al-Deyab S. S., Hammouti B., Bouyanzer A., *Int. J. Electrochem. Sci.* 5 (2010) 1060.

(2016); <http://www.jmaterenvirosci.com/>